PERGAMON

Polyhedron 20 (2001) 2889–2900

POLYHEDRON

www.elsevier.com/locate/poly

Metal complexes of 4′-(3-phenylpropoxy)-2,2′:6′,2″-terpyridine and 4′-(3-propoxy)-2,2′:6′,2″-terpyridine

Xiaoming Liu [a,*], Eric J.L. McInnes [b], Colin A. Kilner [a], Mark Thornton-Pett [a], Malcolm A. Halcrow [a,*]

[a] *School of Chemistry, University of Leeds, Woodhouse Lane, Leeds LS2 9JT, UK*

[b] *Department of Chemistry, CW EPR Service Centre, University of Manchester, Oxford Road, Manchester M13 9PL, UK*

Received 25 May 2001; accepted 3 August 2001

Abstract

Reaction of 4′-chloro-2,2′:6′,2″-terpyridine with 3-phenyl-*n*-propanol or *n*-propanol in the presence of excess KOH in dmso, respectively, yields 4′-(3-phenylpropoxy)-2,2′:6′,2″-terpyridine (L^2) and 4′-(3-propoxy)-2,2′:6′,2″-terpyridine (L^3). The following complexes of these two ligands have been prepared: $[\{Cu(\mu\text{-}Cl)L\}_2](BF_4)_2$, $[Cu(NCMe)(L)](BF_4)_2$, $[PdCl(L)]BF_4$ and $[PtCl(L)]BF_4$ ($L = L^2$, L^3). Recrystallisation of $[Cu(NCMe)(L^2)](BF_4)_2$ from $PhCN/Et_2O$ yields $[Cu(NCPh)(L^2)](BF_4)_2$, whose crystal structure shows a square planar Cu(II) ion with substantial disorder in the PhCN ligand and 3-phenylpropoxy tail. The single crystal structure of $[PdCl(L^2)]BF_4{\cdot}2CH_3NO_2$ contains a square planar Pd(II) centre. Neither of these structures, nor the solution spectroscopic or electrochemical data from the complexes, provide any evidence for intramolecular π–π interactions between the terpyridine ring and phenylpropoxy substituent. (Non-SI unit employed: $1\ G = 10^{-4}$ T.)

Keywords: Cu(II) complexes; UV–Vis; EPR spectra

1. Introduction

We have recently reported a structural and electrochemical study of the complexes $[Cu(L^1)(Tp^R)]BF_4$ (L^1 = 1-{pyrid-2-yl}-3-{2′,5′-dimethoxyphenyl}pyrazole; $[Tp^R]^-$ = *tris*-{3-phenylpyrazolyl}borate $\{[Tp^{Ph}]^-\}$, *tris*-{3-[4-methylphenyl]pyrazolyl}borate $\{[Tp^{Tol}]^-\}$, *tris*-{3-[4-fluorophenyl]pyrazolyl}borate $\{[Tp^{PhF}]^-\}$; Scheme 1), which exhibit an intramolecular π–π interaction involving the dimethoxyphenyl moiety of L^1 and a $[Tp^R]^-$ aryl substituent [1,2]. The cyclic voltammograms of these complexes in CH_2Cl_2/0.5 M $N^nBu_4PF_6$ at room temperature contain a fully reversible one-electron oxidation by cyclic voltammetry, attributable to oxidation of the L^1 dimethoxyphenyl moiety to a radical cation. These are unique examples of heteroarene dimer cation species that are stable enough to be characterised by standard synthetic methods, rather than by pulse radiolysis [3,4].

Following on from this initial work, we were keen to investigate more generally the effects of π–π interactions on the properties of redox-active and/or photoactive arenes and their complexes. Ideally, one should prepare bis-aryl ligands containing intramolecular π–π interactions so as not to rely on serendipitous, and difficult to design, inter-ligand interactions to achieve the desired π–π stacking [1,2,5,6]. As an initial study, we have chosen to investigate terpyridyl ligands bearing tethered aryl substituents, to examine the effects of π–π interactions on the well-known reductive ligand-based electrochemistry and fluorescent behaviour of their Pt(II) complexes [7,8]. This paper describes our initial efforts towards this goal.

* Corresponding authors. Tel.: +44-113-233-6506; fax: +44-113-233-6565.

E-mail address: m.a.halcrow@chem.leeds.ac.uk (X. Liu).

0277-5387/01/$ - see front matter
PII: S0277-5387(01)00905-6

2. Experimental

Unless otherwise stated, all manipulations were carried out in air using commercial grade solvents. 4′-Chloro-2,2′:6′,2″-terpyridine, 3-phenylpropan-1-ol, propan-1-ol, HBF_4 (48 wt.% in water), hydrated $Cu(BF_4)_2$, (Aldrich), $CuCl_2{\cdot}2H_2O$, $PdCl_2$ and K_2PtCl_4 (Avocado) were used as supplied, while 2,6-bis-(pyrid-2-yl)-4-pyridone [9] was prepared by the literature procedures.

2.1. 4′-(3-Phenylpropoxy)-2,2′:6′,2″-terpyridine (L^2)

2.1.1. Method A

Freshly ground KOH (1.40 g, 2.5×10^{-2} mol) was suspended in dmso (20 cm^3), to which 2,6-bis-(pyrid-2-yl)-4-pyridone (0.80 g, 3.2×10^{-3} mol) and 1-bromo-3-phenylpropane (0.80 g, 4.0×10^{-3} mol) were added in that order. The reaction mixture was then stirred for 16 h at 60 °C. Addition of water (20 cm^3) to the resultant orange solution gave a milky suspension, which after standing at −10 °C, yielded a yellowish white solid which was collected and washed with water. The solid was dried over P_2O_5 overnight. Recrystallisation from hot hexane gave a white crystalline solid (yield 0.65 g, 55%).

2.1.2. Method B

The procedure in method A was followed, using 3-phenylpropan-1-ol (0.54 g, 4.0×10^{-3} mol) and 4′-chloro-2,2′:6′,2″-terpyridine (0.86 g, 3.2×10^{-3} mol) (yield 1.1 g, 93%). *Anal.* Found: C, 78.5; H, 5.8; N, 11.7. Calc. for $C_{24}H_{21}N_3O$: C, 78.5; H, 5.8; N, 11.4%. M.p. 103–105 °C. ^{1}H NMR ($CDCl_3$): δ 8.71 (2H, d, $J = 4.8$ Hz, Py $H^{6/6''}$), 8.64 (2H, d, $J = 7.9$ Hz, Py $H^{3/3''}$), 8.05 (2H, s, Py $H^{3'/5'}$), 7.86 (2H, pseudo-t, 7.5 Hz, Py $H^{4/4''}$), 7.32 (7H, m, Py $H^{5/5''}$ + Ph H^{2-5}), 4.25 (2H, t, $J = 6.1$ Hz, OCH_2), 2.88 (2H, t, $J = 7.6$ Hz, $PhCH_2$), 2.20 (2H, dd, $J = 6.1$ and 7.6 Hz, $CH_2CH_2CH_2$). EI MS; m/z: 367 [M^+], 276 [$M - CH_2Ph$]$^+$, 262 [$M - C_2H_4Ph$]$^+$, 248 [$M - C_3H_6Ph$]$^+$, 233 [$M - OC_3H_6Ph + H$]$^+$.

2.2. 4′-(Propoxy)-2,2′:6′,2″-terpyridine (L^3)

Method as for L^2, using 4′-chloro-2,2′:6′,2″-terpyridine (0.86 g, 3.2×10^{-3} mol) and propan-1-ol (0.25 g, 4.2×10^{-3} mol). The product formed colourless needles from hot hexanes (yield 0.74 g, 64%). *Anal.* Found: C, 73.9; H, 6.0; N, 14.6. Calc. for $C_{18}H_{17}N_3O$: C, 73.2; H, 5.8; N, 14.2%. M.p. 105–107 °C. ^{1}H NMR ($CDCl_3$): δ 8.67 (2H, d, $J = 4.8$ Hz, Py $H^{6/6''}$), 8.61 (2H, d, $J = 8.0$ Hz, Py $H^{3/3''}$), 7.98 (2H, s, Py $H^{3'/5'}$), 7.92 (2H, dd, $J = 7.6$ and 8.0 Hz, Py $H^{4/4''}$), 7.42 (2H, d, $J = 7.6$ Hz, Py $H^{5/5''}$), 4.18 (2H, t, $J = 6.5$ Hz, OCH_2), 1.73 (2H, m, $CH_2CH_2CH_3$), 1.07 (3H, t, $J = 7.5$ Hz, CH_3). EI MS; m/z: 291 [M^+], 276 [$M - CH_3$]$^+$, 262 [$M - C_2H_5$]$^+$, 248 [$M - C_3H_7$]$^+$, 233 [$M - OC_3H_7 + H$]$^+$.

2.3. 4′-(3-Phenylpropoxy)-2,2′:6′,2″-terpyridindionium ditetrafluoroborate ($[H_2L^2][BF_4]_2$)

A mixture of L^2 (0.50 g, 1.4×10^{-3} mol) and aqueous HBF_4 (0.76 cm^3 of a 5.5 M solution, 4.2×10^{-3} mol) in MeOH (10 cm^3) was allowed to evaporate slowly, yielding colourless crystals (yield 0.44 g, 58%). *Anal.* Found: C, 53.2; H, 4.3; N, 7.6. Calc. for $C_{24}H_{23}B_2F_8N_3O$: C, 53.1; H, 4.3; N, 7.7%. ^{1}H NMR ($\{CD_3\}_2SO$): δ 8.87 (4H, m, Py $H^{6/6''}$ + Py $H^{3/3''}$), 8.38 (2H, pseudo-t, 7.7 Hz, Py $H^{4/4''}$), 8.16 (2H, s, Py $H^{3'/5'}$), 7.82 (2H, pseudo-t, 7.5 Hz, Py $H^{5/5''}$), 7.27 (5H, m, Ph H^{2-5}), 4.33 (2H, t, $J = 6.3$ Hz, OCH_2), 2.81 (2H, t, $J = 7.3$ Hz, $PhCH_2$), 2.12 (2H, dd, $J = 6.3$ and 7.3 Hz, $CH_2CH_2CH_2$).

2.4. $[PdCl(L^2)]BF_4$ (1)

A suspension of $PdCl_2$ (0.08 g, 5.0×10^{-4} mol), L^2 (0.18 g, 5.0×10^{-4} mol) and $NaBF_4$ (0.17 g, 1.5×10^{-3} mol) were suspended in $MeNO_2$ (10 cm^3). This mixture was refluxed for 5 h. Insoluble solid was filtered off and the filtrate was reduced to approximately 2 cm^3 volume. Vapour diffusion of Et_2O into this solution gave a pale yellow crystalline solid (yield 0.27 g, 90%). *Anal.*

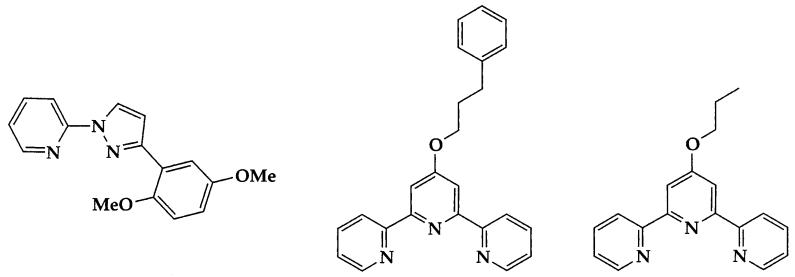

L^1 L^2 L^3

Scheme 1.

Found: C, 47.3; H, 3.5; N, 6.8. Calc. for $C_{24}H_{21}BClF_4N_3OPd$: C, 48.3; H, 3.5; N, 7.0%. FAB MS; m/z: 508 ($[^{106}Pd^{35}Cl(L^2)]^+$), 473 ($[^{106}Pd(L^2)]^+$), 354 ($[^{106}Pd(L^2–C_3H_6C_6H_5)]^+$ with correct isotopic distributions.

2.5. $[PdCl(L^3)]BF_4$ (2)

Method as for **1**, using L^3 (0.15 g, 5.0×10^{-4} mol). The product is a pale yellow solid (yield 0.23 g, 89%). *Anal.* Found: C, 41.6; H, 3.5; N, 7.9. Calc. for $C_{18}H_{17}BClF_4N_3OPd$: C, 41.6; H, 3.3; N, 8.1%. FAB MS; m/z: 432 $[^{106}Pd^{35}Cl(L^3)]^+$, 397 $[^{106}Pd(L^3)]^+$, 354 $[^{106}Pd(L^3–C_3H_7)]^+$ with correct isotopic distributions.

2.6. $[PtCl(L^2)]BF_4$ (3)

A suspension of K_2PtCl_4 (0.21 g, 5.0×10^{-4} mol), L^2 (0.18 g, 5.0×10^{-4} mol) and $NaBF_4$ (0.11 g, 1.0×10^{-3} mol) in $MeNO_2$ (20 cm^3) was refluxed for 21 h. The NaCl precipitate was removed by hot filtration, and the filtrate was concentrated. Addition of Et_2O to this solution afforded a red solid which was collected, washed with diethyl ether and dried in vacuo (yield 0.17 g, 50%). *Anal.* Found: C, 41.3; H, 3.6; N, 5.9. Calc. for $C_{24}H_{21}BClF_4N_3OPt$: C, 41.0; H, 3.3; N, 6.0%. FAB MS; m/z: 597 $[^{195}Pt^{35}Cl(L^2)]^+$, 478 $[^{195}Pt^{35}Cl(L^2–C_3H_6C_6H_5)]^+$, 443 $[^{195}Pt(L^2–C_3H_6C_6H_5)]^+$ with correct isotopic distributions.

2.7. $[PtCl(L^3)]BF_4$ (4)

Method as for **3**, using L^3 (0.15 g, 5.0×10^{-4} mol). The product was a red microcrystalline solid (yield 0.16 g, 53%). *Anal.* Found: C, 35.7; H, 2.9; N, 6.6. Calc. for $C_{18}H_{17}BClF_4N_3OPt$: C, 35.5; H, 2.8; N, 6.9%. FAB MS; m/z: 521 $[^{195}Pt^{35}Cl(L^3)]^+$, 486 $[^{195}Pt(L^3)]^+$, 478 $[^{195}Pt^{35}Cl(L^3–C_3H_7)]^+$, 443 $[^{195}Pt(L^3–C_3H_7)]^+$ with correct isotopic distributions.

2.8. $[\{Cu(\mu\text{-}Cl)(L^2)\}_2](BF_4)_2$ (5)

A mixture of $CuCl_2 \cdot 2H_2O$ (0.085 g, 5.0×10^{-4} mol), L^2 (0.18 g, 5.0×10^{-4} mol) and $NaBF_4$ (0.055 g, 5.0×10^{-4} mol) was refluxed in $MeNO_2$ (20 cm^3) for 4 h. The pale blue solution was filtered and concentrated to approximately 2 cm^3, and the product precipitated with Et_2O. Vapour diffusion of Et_2O into a solution of the complex in MeCN yielded blue microcrystals (yield 0.21 g, 75%). *Anal.* Found: C, 52.2; H, 3.9; N, 7.6. Calc. for $C_{48}H_{42}B_2Cl_2Cu_2F_8N_6O_2$: C, 52.1; H, 3.8; N, 7.6%. FAB MS; m/z: 1017 $[^{63}Cu_2^{35}Cl_2(L^2)_2^{11}BF_4]^+$, 465 $[^{63}Cu^{35}Cl(L^2)]^+$, 449 $[^{63}CuF(L^2)]^+$, 430 $[^{63}Cu(L^2)]^+$, 311 $[^{63}Cu(L^2–C_3H_6C_6H_5)]^+$ with correct isotopic distributions.

2.9. $[\{Cu(\mu\text{-}Cl)(L^3)\}_2](BF_4)_2$ (6)

Method as for **5**, using L^3 (0.15 g, 5.0×10^{-4} mol). The product formed blue needles from $MeCN/Et_2O$ (yield 0.23 g, 98%). *Anal.* Found: C, 45.4; H, 3.7; N, 9.0. Calc. for $C_{36}H_{34}B_2Cl_2Cu_2F_8N_6O_2$: C, 45.3; H, 3.6; N, 8.8%. FAB MS; m/z: 865 $[^{63}Cu_2^{35}Cl_2(L^3)_2^{11}BF_4]^+$, 389 $[^{63}Cu^{35}Cl(L^3)]^+$, 373 $[^{63}CuF(L^3)]^+$, 354 $[^{63}Cu(L^3)]^+$, 311 $[^{63}Cu(L^3–C_3H_7)]^+$ with correct isotopic distributions.

2.10. $[Cu(NCMe)(L^2)](BF_4)_2$ (7)

A solution of $Cu(BF_4)_2 \cdot 6H_2O$ (0.70 g, 2.0×10^{-3} mol) and L^2 (0.73 g, 2.0×10^{-3} mol) in MeCN (20 cm^3) was stirred at room temperature for 1 h. The blue solution was filtered and concentrated to approximately 5 cm^3, resulting in the precipitation of a blue solid. Slow addition of Et_2O to the mixture afforded further precipitation. The solid was collected, washed with Et_2O and dried in vacuo. Recrystallisation by vapour diffusion of Et_2O into a MeCN solution of the complex afforded a blue–purple crystalline solid (yield 1.00 g, 77%). *Anal.* Found: C, 48.4; H, 3.8; N, 8.6. Calc. for $C_{26}H_{24}B_2CuF_8N_4O$: C, 48.4; H, 3.7; N, 8.7%. FAB MS; m/z: 449 $[^{63}CuF(L^2)]^+$, 430 $[^{63}Cu(L^2)]^+$, 311 $[^{63}Cu(L^2–C_3H_6C_6H_5)]^+$ with correct isotopic distributions. IR spectrum (cm^{-1}, Nujol mull): 2324w, 2297w.

2.11. $[Cu(NCMe)(L^3)](BF_4)_2$ (8)

Method as for **7**, using L^3 (0.60 g, 2.0×10^{-3} mol). The complex formed deep blue microcrystals from $MeCN/Et_2O$ (yield 0.96 g, 84%). *Anal.* Found: C, 42.0; H, 3.6; N, 9.8. Calc. for $C_{20}H_{20}B_2CuF_8N_4O$: C, 42.2; H, 3.5; N, 9.8%. FAB MS: m/z 373 $[^{63}CuF(L^3)]^+$, 354 $[^{63}Cu(L^3)]^+$, 311 $[^{63}Cu(L^3–C_3H_7)]^+$ with correct isotopic distributions. IR spectrum (cm^{-1}, Nujol mull): 2331w, 2301w.

2.12. Single crystal X-ray structure determinations

Yellow blocks of $[PdCl(L^2)]BF_4 \cdot 2CH_3NO_2$-($1.2CH_3NO_2$) were obtained from a hot $MeNO_2$ solution of the complex. Storage of a benzonitrile solution of **7** at −30 °C yielded blue crystals of formula $[Cu(NCPh)(L^2)](BF_4)_2$ (**9**: *Anal.* Found: C, 53.4; H, 3.9; N, 8.2. Calc. for $C_{31}H_{26}B_2CuF_8N_4O$: C, 52.6; H, 3.7; N, 7.9%). Experimental details from the structure determinations are given in Table 1. Both structures were solved by standard heavy atom methods (SHELXS-97 [10]) and refined by full-matrix least-squares on F^2 (SHELXL-97 [11]).

Table 1
Crystal data and structure refinement parameters for $[PdCl(L^1)]BF_4{\cdot}2CH_3NO_2$ ($1.2CH_3NO_2$) and $[Cu(NCPh)(L^1)](BF_4)_2$ (**9**)

	$[PdCl(L^1)]BF_4{\cdot}2CH_3NO_2$ ($1.2CH_3NO_2$)	$[Cu(NCPh)(L^1)](BF_4)_2$ (**9**)
Empirical formula	$C_{26}H_{27}BClF_4N_5O_5Pd$	$C_{31}H_{26}B_2CuF_8N_4O$
Formula weight	718.19	707.72
Temperature (K)	150(2)	293(2)
λ (Å)	0.71073	0.71073
Crystal habit	yellow block	blue lath
Crystal size (mm)	$0.75\times0.51\times0.36$	$0.24\times0.13\times0.07$
Crystal class	orthorhombic	triclinic
Space group	$Pna2_1$	$P\bar{1}$
Unit cell dimensions		
a (Å)	19.3958(6)	13.0402(3)
b (Å)	22.8909(5)	13.8065(4)
c (Å)	6.6562(1)	8.6891(3)
α (°)		87.6469(16)
β (°)		83.2172(18)
γ (°)		76.7599(17)
V (Å^3)	2955.27(12)	1511.98(8)
Z	4	2
μ (Mo Kα) (mm^{-1})	0.789	0.805
Diffractometer	Enraf–Nonius KappaCCD	Enraf–Nonius KappaCCD
Measured reflections	19 947	24 570
Independent reflections	6431	6865
R_{int}	0.087	0.053
Absorption correction	multi-scan	multi-scan
Min/max transmission	0.589, 0.764	0.830, 0.946
Observed reflections ($I>2\sigma(I)$)	5567	5666
Range in 2θ (°)	$5.50<\theta<54.98$	$5.52<\theta<54.94$
Index ranges	$-24<h<25,\ -29<k<27,\ -8<l<8$	$-16<h<16,\ -17<k<17,\ -11<l<11$
Number of parameters	396	583
Number of restraints	7	182
$R(F)$ [a], $wR(F^2)$ [b]	0.055, 0.150	0.044, 0.116
Goodness-of-fit on F^2	1.038	1.023
Weighting scheme [c]	$w=1/[\sigma^2(F_o^2)+(0.0854P)^2+3.3986P]$	$w=1/[\sigma^2(F_o^2)+(0.0565P)^2+0.6657P]$
Max. shift/e.s.d.	0.051	0.017
$\Delta\rho_{min}$, $\Delta\rho_{max}$	−1.41, 0.58	−0.87, 0.42
Flack parameter	0.39(7)	

[a] $R=\Sigma[|F_o|-|F_c|]/\Sigma|F_o|$.
[b] $wR=[\Sigma w(F_o^2-F_c^2)/\Sigma wF_o^4]^{1/2}$.
[c] $P=(F_o^2+2F_c^2)/3$.

2.13. X-ray structure determination of $[PdCl(L^2)]BF_4{\cdot}2CH_3NO_2(1.2CH_3NO_2)$

This crystal was refined as a racemic twin. No disorder was detected in the complex cation or the anion. However, the O atoms of the solvent molecule centred on N(41) were disordered over three equally occupied orientations, with all N–O distances restrained to 1.27(2) Å. All wholly occupied non-H atoms with occupancy ≥ 0.5 were refined anisotropically, and all H atoms were placed in calculated positions.

2.14. X-ray structure determination of $[Cu(NCPh)(L^2)](BF_4)_2$ (**9**)

Both ligands in the complex cation, and one of the BF_4^- anions, suffer from disorder. The phenyl ring of the benzonitrile ligand is disordered over two equally occupied orientations C(33A)–C(37A) and C(33B)–C(37B), by rotation about the bridgehead atom C(32). All C–C bonds within both phenyl rings were constrained to be the same. The L^2 3-phenylpropoxy substituent is also disordered over two different conformations O(20A)–C(29A) and O(20B)–C(29B), which were also modelled as equally occupied. Equivalent C–O or C–C bond lengths in each conformation were constrained to be the same. The anion centred on B(43) is disordered by rotation about the B(43)–F(44) bond. Three orientations of this anion were modeled, with all B–F distances constrained to be the same: F(45A)–F(47A), with occupancy 0.5; and F(45B)–F(47B) and F(45C)–F(47C), each with occupancy 0.25. All the constraints in the final model had a sum of 0.03 Å. All wholly occupied non-H atoms with occupancy ≥ 0.5 were refined anisotropically, and H atoms were placed in calculated positions.

2.15. Other measurements

Infra-red spectra were obtained as Nujol mulls pressed between KBr windows, or in NaCl solution cells, between 400 and 4000 cm^{-1} using a Nicolet Avatar 360 spectrophotometer. UV–Vis spectra were obtained with a Perkin–Elmer Lambda 900 spectrophotometer operating between 200 and 1100 nm, in 1 cm quartz cells. All NMR spectra were run on a Bruker ARX250 spectrometer, operating at 250.1 MHz (^1H) and 62.9 MHz (^{13}C). Mass spectra were performed on a VG AutoSpec spectrometer, the fast atom bombardment spectra employing a 3-NOBA matrix. CHN microanalyses were performed by the University of Leeds School of Chemistry microanalytical service. EPR spectra were obtained using a Bruker ESP300E spectrometer; X-band spectra (approximately 9.5 GHz) employed an ER4102ST resonator and ER4111VT cryostat, while for S-band spectra (approximately 4 GHz) a ER4118SM-S-5W1 resonator and a ER4118VT cryostat were used. Melting points are uncorrected.

Conductivity measurements were obtained with a Jenway 4310 analyser, at a concentration of 1.0×10^{-3} mol dm^{-3}. All electrochemical measurements were carried out using an Autolab PGSTAT30 voltammetric analyser, in CH_2Cl_2 containing 0.5 M $N^nBu_4BF_4$ (prepared from N^nBu_4OH and aqueous HBF_4 in water, followed by two recrystallisations from hot MeOH) as supporting electrolyte. Voltammetric experiments involved the use of platinum disk working and platinum wire counter electrodes, and an Ag/AgCl reference electrode. All potentials quoted are referenced to an internal ferrocene/ferrocenium standard and were obtained at a scan rate of 100 mV s^{-1}, unless otherwise stated.

3. Results and discussion

Molecular models suggested that a 4-atom chain between two aryl groups is an optimum length to allow a geometrically favourable π–π interaction [12] to form between the linked rings. With this in mind, the ligand 4′-(3-phenyl-*n*-propoxy)-2,2′:6′,2″-terpyridine (L^2) was synthesised either from 3-phenylpropan-1-ol and 4′-chloro-2,2′:6′,2″-terpyridine, or from 1-bromo-3-phenylpropane and 2,6-(pyrid-2-yl)pyrid-4-one, in a KOH/dmso suspension according to the method of Constable and Newkome [13,14]. For comparison, an equivalent ligand lacking a phenyl substituent, 4′-propoxy-2,2′:6′,2″-terpyridine (L^3), was also prepared by an analogous synthesis using 4′-chloro-2,2′:6′,2″-terpyridine and propan-1-ol. Both ligands were isolated from the reaction mixtures by precipitation with water, yielding white solids that were recrystallised from hot hexanes. The complexes $[PdCl(L)]BF_4$ ($L = L^2$, **1**; $L = L^3$, **2**) $[PtCl(L)]BF_4$ ($L = L^2$, **3**; $L = L^3$, **4**) and $[Cu-Cl(L)]BF_4$ ($L = L^2$, **5**; $L = L^3$, **6**) were prepared from these ligands, using similar synthetic methods to those previously reported for $[MCl(terpy)]^+$ (M = Cu, Pd, Pt) compounds [15–17]. The complexes $[Cu(NCMe)(L)](BF_4)_2$ ($L = L^2$, **7**; $L = L^3$, **8**) were also synthesised, by complexation of the appropriate tridentate ligand with 1 molar equivalent of hydrated $Cu(BF_4)_2$ in MeCN.

Microanalyses for all of the complexes were consistent with the proposed formulations, while the IR spectra of **1**–**6** showed the presence of BF_4^- and the appropriate tridentate ligand only. For **7** and **8** additional IR absorptions were exhibited corresponding to the $\nu_{C\equiv N}$ vibration of the MeCN ligand (for **7**, $\nu_{C\equiv N}$ = 2324, 2297 cm^{-1}; for **8**, $\nu_{C\equiv N}$ = 2331, 2301 cm^{-1}) [18]. However, while precedent suggests that **1**–**4** and **7** and **8** can safely be described as mononuclear complexes, **5** or **6** could in principle exist as monomeric complexes, or as $[\{Cu(\mu\text{-}Cl)(L)\}_2](BF_4)_2$ ($L = L^2$, L^3) dimers analogous to the crystallographically characterised $[\{Cu(\mu\text{-}Cl)(terpy)\}_2](PF_6)_2$ [15]. The latter possibility is favoured by the FAB MS of these two compounds, which exhibit weak molecular ions corresponding to $[\{^{63}Cu(\mu\text{-}^{35}Cl)(L)\}_2(^{11}BF_4)]^+$ ($L = L^2$, $M^+ = 1017$; $L = L^3$, $M^+ = 865$); none of the other complexes exhibit dimer peaks by mass spectrometry. The dimeric molecular structures of **5** and **6** were confirmed by the spectroscopic studies described below.

Single crystals of X-ray quality of formula $[PdCl(L^2)]BF_4{\cdot}2CH_3NO_2$ ($1.2CH_3NO_2$) were grown by vapour diffusion of Et_2O into a $MeNO_2$ solution of the complex. Recrystallisation of $[Cu(NCMe)(L^2)](BF_4)_2$ from $PhCN/Et_2O$ yielded deep blue crystals analysing as $[Cu(NCPh)(L^2)](BF_4)_2$ (**9**). The presence of PhCN in these crystals was suggested by both microanalysis and IR spectroscopy ($\nu_{C\equiv N}$ = 2279, 2226 cm^{-1}) [18], and subsequently confirmed by the crystal structure analysis described below. Views of the molecular structures of these two complexes in the crystal are shown in Figs. 1 and 3, while selected metric parameters are given in Tables 2–4.

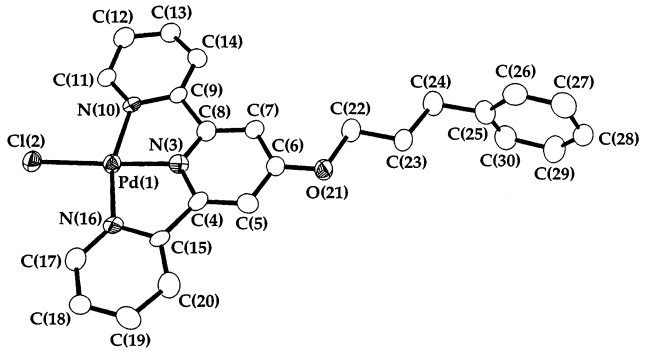

Fig. 1. Solid state structure of the complex cation in the crystal of $[PdCl(L^2)]BF_4{\cdot}2CH_3NO_2(1.2CH_3NO_2)$, showing the atom numbering scheme employed. For clarity, all hydrogen atoms have been omitted.

Table 2
Selected bond lengths (Å) and bond angles (°) for the structure of $[PdCl(L^2)]BF_4{\cdot}2CH_3NO_2$ ($1.2CH_3NO_2$)

Bond lengths	
Pd(1)–Cl(2)	2.2948(10)
Pd(1)–N(3)	1.924(4)
Pd(1)–N(10)	2.035(3)
Pd(1)–N(16)	2.036(3)
Bond angles	
Cl(2)–Pd(1)–N(3)	178.1(3)
Cl(2)–Pd(1)–N(10)	98.02(10)
Cl(2)–Pd(1)–N(16)	100.28(11)
N(3)–Pd(1)–N(10)	81.46(14)
N(3)–Pd(1)–N(16)	80.16(15)
N(10)–Pd(1)–N(16)	161.49(16)

Table 3
Selected bond lengths (Å) and bond angles (°) for the structure of $[Cu(NCPh)(L^1)](BF_4)_2$ (**9**)

Bond lengths	
Cu(1)–N(2)	1.908(2)
Cu(1)–N(9)	2.021(2)
Cu(1)–N(15)	2.023(2)
Cu(1)–N(30)	1.949(2)
Cu(1)–F(39)	2.4981(15)
Cu(1)–F(44)	2.3712(15)
Bond angles	
N(2)–Cu(1)–N(9)	80.55(8)
N(2)–Cu(1)–N(15)	80.50(8)
N(2)–Cu(1)–N(30)	171.99(8)
N(2)–Cu(1)–F(39)	86.38(7)
N(2)–Cu(1)–F(44)	97.32(7)
N(9)–Cu(1)–N(15)	161.04(8)
N(9)–Cu(1)–N(30)	99.82(8)
N(9)–Cu(1)–F(39)	87.43(7)
N(9)–Cu(1)–F(44)	93.72(7)
N(15)–Cu(1)–N(30)	98.99(8)
N(15)–Cu(1)–F(39)	91.70(7)
N(15)–Cu(1)–F(44)	88.37(7)
N(30)–Cu(1)–F(39)	85.65(7)
N(30)–Cu(1)–F(44)	90.65(7)
F(39)–Cu(1)–F(44)	176.26(6)

The asymmetric unit of $1.2CH_3NO_2$ contains one complex cation lying on a general position, with one anion and two lattice solvent molecules that do not interact with the metal centre. The coordination at Pd(1) is essentially planar (Table 2, Fig. 1), the Pd(1)–N bond lengths and Cl–Pd(1)–N and N–Pd(1)–N angles being within the ranges found for other $[PdX(terpy)]^+$ (X^- = halide, pseudohalide or alkyl anion) complexes [19]. The L^2 3-phenylpropoxy substituent adopts a single conformation in the crystal, with all CH_2 groups being *anti* to each other.

The cations in $1.2CH_3NO_2$ pack into stacks (Fig. 2), each molecule within the stack being related by $2-x$, $1-y$, $-1/2+z$. Within these columns of cations, each molecule is separated by Pd(1)···Pd(1′) = 3.459(1) Å while the dihedral angle between the least-squares planes of the terpyridyl skeletons on adjacent molecules, [N(3)–C(19)] and [N(3′)–C(19′)], is 0.9(2)°. There is an edge-to-face C–H–π interaction between H(12) of one molecule and the phenyl substituent of a neighbouring cation [C(25″)–C(30)″] related by $-1/2+x$, $3/2-y$, z, with H(12)–X(1″) = 2.5 Å and C(12)–H(12)···X(1″) = 157° [X(1″) = centroid of C(25″)–C(30″)]. The phenyl substituent of each cation [C(25)–C(30)] also forms a π–π interaction with that of the neighbouring cation [C(25‴)–C(30‴)] related by $2-x$, $2-y$, $-1/2+z$, the dihedral angle between the two rings being 1.7(2)°, the inter-planar distance 3.1 Å and the centroids of the two rings being offset by 4.5 Å [12].

Table 4
Unfavourable intermolecular H···H and H···F distances (Å) involving the disordered regions of the crystal structure of $[Cu(NCPh)(L^1)](BF_4)_2$ (**9**)

	Symmetry relation	$d_{H\cdots X}$ [a] (Å)
H(21D)···H(35B′)	x, $1+y$, z	2.3
H(25A)···H(36B′)	$2-x$, $2-y$, $2-z$	2.0
H(25A)···H(37B″)	$2-x$, $2-y$, $2-z$	1.6
H(25B)···H(33B‴)	$2-x$, $2-y$, $1-z$	2.2
H(26A)···H(35A⁗)	$1+x$, $1+y$, z	2.1
H(26B)···H(27A⁗)	$3-x$, $3-y$, $1-z$	2.2
H(35A)···H(36A⁗)	$1-x$, $1-y$, $2-z$	1.7
H(25B)···F(45C⁗)	$1+x$, y, z	2.5
H(25B)···F(46A⁗)	$1+x$, y, z	2.5
H(25B)···F(46C⁗)	$1+x$, y, z	2.4
H(33B)···F(46A⁗)	$1-x$, $2-y$, $1-z$	2.5
H(33B)···F(46C⁗)	$1-x$, $2-y$, $1-z$	2.5
H(37A)···F(45B⁗)	$1-x$, $2-y$, $2-z$	2.3

All contacts are shorter than the sum of the van der Waals radii of two H atoms (2.4 Å), or of a H atom and a F atom (2.6 Å) [21].
[a] X = H, F

The Cu ion in **9** is almost perfectly planar, with Cu···N distances that are normal for tetragonal Cu(II) species [20]. There is one long Cu···F contact to each anion [Cu(1)–F(39) = 2.4981(15), Cu(1)–F(44) = 2.3712(15) Å], leading to a distorted octahedral [4 + 1 + 1] coordination sphere (Table 3, Fig. 3). In contrast to the structure of **1**, the L^2 3-phenylpropoxy group in **9** is disordered over two equally occupied conformations. In one conformation [O(20A)–C(29A)] the propoxy tether exhibits exclusively *anti* X–C–C–C (X = C, O) torsion angles, while the other conformation [O(20B)–C(29B)] contains a *gauche* C(21B)–C(22B)–C(23B)–C(24B) torsion. The PhCN phenyl substituent is also disordered over two equally occupied orientations [C(33A)–C(37A) and C(33B)–C(37)B], by rotation about the C(31)–C(32) bond. Finally, the anion centred on B(43) is disordered over three orientations by rotation about the B(43)–F(44) bond.

Adjacent molecules in the lattice of **9** interact by van der Waals contacts only. The packing diagram of this structure reveals several unfavourable intermolecular

H···H contacts between individual disorder orientations of neighbouring cations (Table 4). Clearly, therefore, the conformation of any individual molecule in the lattice will be dictated by those adopted by its neighbours. There are also several close intermolecular H···F contacts from the disordered regions of the cation to the disordered anion of neighbouring molecules (Table 4), so that the anion disorder in this structure is dictated, at least in part, by the ligand disorder.

Conductivity measurements of the complexes in this study were run in MeCN (Table 5). Complexes **1**–**6** exhibit conductivities in the range 89–110 $\Omega^{-1}\,cm^2\,mol^{-1}$ (per mole of empirical formula units), while those of **7** and **8** are larger at approximately 190 $\Omega^{-1}\,cm^2\,mol^{-1}$. These data are all somewhat smaller than the 'typical' values quoted for a 1:1 (140 $\Omega^{-1}\,cm^2\,mol^{-1}$) or 2:1 (220 $\Omega^{-1}\,cm^2\,mol^{-1}$) electrolyte in MeCN [22], which may reflect some ion pairing in solution. However, from comparison with **1**–**4** it seems clear that **7** and **8** are better described as 2:1 electrolytes, and that the chloride ligands in **5** and **6** remain coordinated to the Cu atoms. As discussed below, **5** and **6** are in fact better described as 2:1 electrolytes, $[\{Cu(\mu\text{-}Cl)L\}_2](BF_4)_2$ ($L = L^2$, L^3).

UV–Vis data for the ligands and complexes were run in MeCN at 290 K, and are listed in Table 5. It is clear

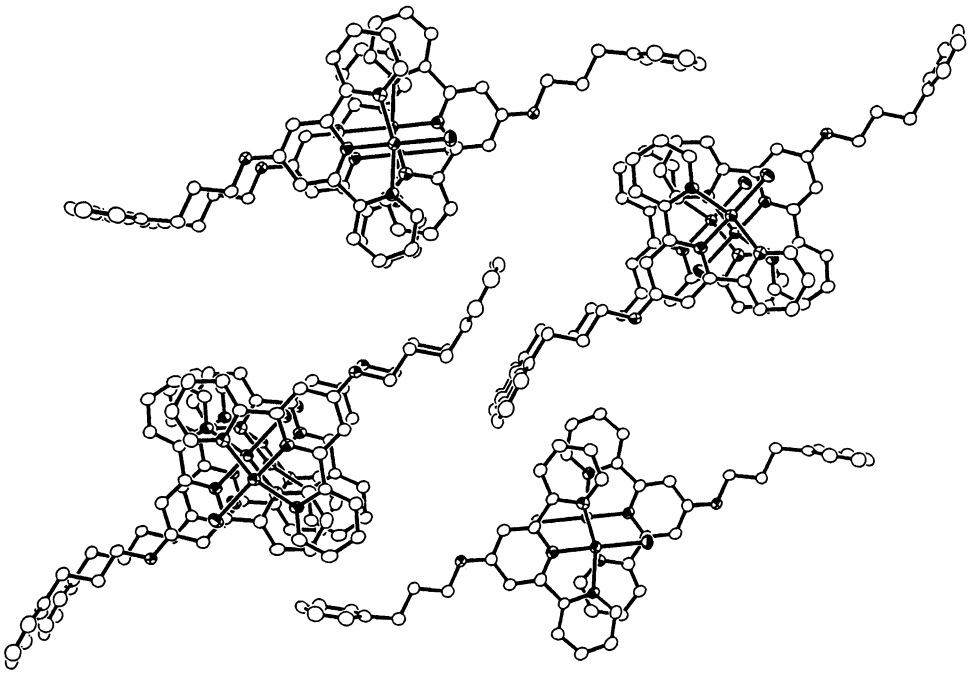

Fig. 2. Partial packing diagram for $[PdCl(L^2)]BF_4{\cdot}2CH_3NO_2(1.2CH_3NO_2)$, showing the arrangement of cations into 1D stacks. For clarity all hydrogen atoms, anions and solvent molecules have been omitted.

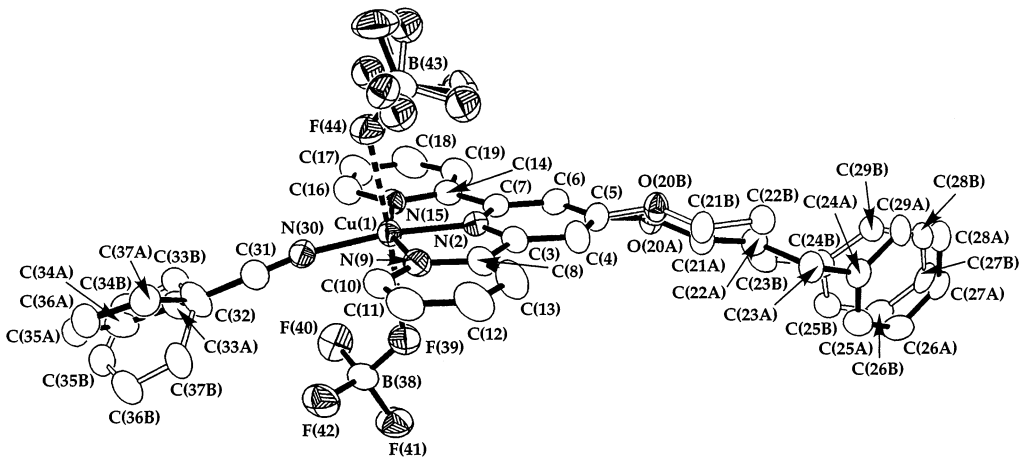

Fig. 3. Solid state structure of the complex molecule in the crystal of $[Cu(NCPh)(L^2)](BF_4)_2$ (**9**) showing the atom numbering scheme employed. All orientations of the disordered ligands and anion are shown (see Section 2). For clarity, all hydrogen atoms have been omitted, while the numbers of disordered F atoms are not shown.

Table 5
Conductivity and UV–Vis spectroscopic data for the compounds in this study (MeCN, 290 K) [a]

	Λ_M, (Ω^{-1} cm^2 mol^{-1})	λ_{max}, nm (ε_{max}, 10^3 M cm^{-1})
L^2		240 (23.7), 277 (21.1)
L^3		241 (26.8), 277 (24.7)
$[PdCl(L^2)]BF_4$ (**1**)	93	243 (31.0), 281 (29.3), 333 (sh), 350 (sh)
$[PdCl(L^3)]BF_4$ (**2**)	103	243 (32.2), 281 (28.8), 302 (sh), 333 (sh), 350 (sh)
$[PtCl(L^2)]BF_4$ (**3**)	89	225 (27.8), 255 (26.5), 284 (37.2), 303 (14.3), 316 (14.3), 330 (17.5), 395 (3.9)
$[PtCl(L^3)]BF_4$ (**4**)	110	226 (27.2), 256 (35.3), 284 (33.9), 304 (14.2), 316 (14.7), 330 (17.7), 392 (3.9)
$[\{Cu(\mu\text{-}Cl)(L^2)\}_2](BF_4)_2$ (**5**)	196 [a]	241 (27.8), 263 (33.73), 276 (30.2), 316 (12.1), 328 (11.1), 692 (0.12)
$[\{Cu(\mu\text{-}Cl)(L^3)\}_2](BF_4)_2$ (**6**)	196 [a]	224 (36.2), 263 (31.6), 275 (28.2), 317 (12.1), 328 (11.2), 693 (0.12)
$[Cu(NCMe)(L^2)](BF_4)_2$ (**7**)	199	242 (29.0), 250 (sh), 260 (27.8) 277 (28.6), 316 (12.1), 329 (12.2), 625 (0.13)
$[Cu(NCMe)(L^3)](BF_4)_2$ (**8**)	188	242 (29.3), 251 (28.0), 260 (27.8), 277 (28.8), 317 (12.8), 329 (12.8), 629 (0.13)

[a] For comparison with **1**–**4**, conductivity values calculated per mole of copper ion are $\Lambda_M = 98$ Ω^{-1} cm^2 mol^{-1}; see text.

that the spectra of each pair of complexes (**1**/**2**, **3**/**4**, **5**/**6** and **7**/**8**) are essentially identical, showing differences within each pair that are small-to-insignificant. This strongly implies that the presence of the potentially π–π stacking pendant arm in the L^2-containing complexes has an undetectable effect on their electronic structures. The Cu(II) complexes **5**–**8** each exhibit a single well-defined d–d band. This lies at approximately 65 nm shorter wavelength for **5** and **6**, compared to **7** and **8**, which is inconsistent with the relative positions of Cl^- and MeCN in the spectrochemical series [23] and suggests that the molecular structures of **5**/**6** and **7**/**8** are not comparable.

X-band EPR spectra of the Cu(II) complexes were run as powders, and in frozen 10:1 MeCN–toluene solution (Table 6). Interestingly in the light of their similar solution UV–Vis spectra, the EPR spectra of solid **5** and **6** are markedly different. Both compounds show the $g_\parallel > g_\perp > g_e$ pattern that is typical of tetragonal Cu(II) ions with a $\{d_{x^2-y^2}\}^1$ or $\{d_{xy}\}^1$ ground state [24], but with different g-values. In addition, while the spectrum of **5** is essentially invariant between 290 and 120 K, the spectrum of **6** changes markedly from being axial at 290 K, to rhombic at 120 K. For **6** only, a weak 'half-field' resonance near 1500 G is also apparent, which arises from a $\Delta m_S = \pm 2$ transition and is a characteristic of an exchange-coupled dicopper species with negligible zero-field splitting [24]. This observation was confirmed by re-running the spectrum at S-band, which shows the expected increase in relative intensity of this signal, which now resonates near 600 G. In frozen solution, **5** and **6** give visually identical, broadened spectra in which the $g_\parallel$ component is too broad to be resolved. At S-band only, 'half-field' resonances are also observed in the solution spectra of both compounds at 120 K.

The EPR spectra of **7** in the solid and in frozen solution are well resolved and very similar (Table 6), and are consistent with the presence of isolated, tetragonal Cu(II) centres [24]. The solution spectrum of **8** closely resembles that of **7**, showing that the molecular structures of the two compounds in solution are essentially the same. The powder spectra of **8** and **9** visually resemble that of **7** but are broader, so that the $g_\parallel$ component cannot be unambiguously resolved.

From these spectroscopic and conductivity data, we conclude that **7** and **8** adopt mononuclear structures analogous to crystalline **9**, based on the tetragonal $[Cu(NCMe)L]^{2+}$ ($L = L^2$, L^3) dication. For **5** and **6**, we

Table 6
X-band EPR data for the Cu(II) complexes in this study

		g_1	g_2	g_3	A_1
$[\{Cu(\mu\text{-}Cl)(L^2)\}_2](BF_4)_2$ (**5**)	Powder [a]	2.259	2.052	2.052	
	MeCN [a]		2.063	2.063	
$[\{Cu(\mu\text{-}Cl)(L^3)\}_2](BF_4)_2$ (**6**)	Powder [b]	2.178	2.056	2.056	
	Powder [a]	2.182	2.058	2.028	
	MeCN [a]		2.057	2.057	
$[Cu(NCMe)(L^2)](BF_4)_2$ (**7**)	Powder	2.185	2.056	2.056	171
	MeCN	2.181	2.058	2.058	186
$[Cu(NCMe)(L^3)](BF_4)_2$ (**8**)	Powder		2.057	2.057	
	MeCN	2.193	2.059	2.059	193
$[Cu(NCPh)(L^2)](BF_4)_2$ (**9**)	Powder		2.056	2.056	

Unless otherwise stated, all spectra were obtained at 120 K. Hyperfine couplings are to ^{63,65}Cu and are in G.
[a] Spectrum exhibits an additional 'half-field' resonance near 1500 G (X-band) and/or 600 G (S-band); see text.
[b] Spectrum run at 290 K.

Table 7
Voltammetric data for the compounds in this study

	Solvent	M(II/I) $E_{1/2}$ (V)	M(I/0) E_{pc} (V)	L/L$^-$ $E_{1/2}$ (V)	L$^-$/L^{2-} $E_{1/2}$ (V)
$[H_2L^2](BF_4)_2$	CH_2Cl_2			−0.92	
$[PdCl(L^2)]BF_4$ (**1**)	dmf			−1.20 [a,b]	
$[PdCl(L^3)]BF_4$ (**2**)	dmf			−1.20 [a,b]	
$[PtCl(L^2)]BF_4$ (**3**)	dmf	−1.83		−1.35	−2.45 [b]
$[PtCl(L^3)]BF_4$ (**4**)	dmf	−1.84		−1.36	−2.49 [b]
$[\{Cu(\mu\text{-}Cl)(L^2)\}_2](BF_4)_2$ (**5**)	MeCN	−0.58 [a]	−0.99 [a]	−0.70	
$[\{Cu(\mu\text{-}Cl)(L^3)\}_2](BF_4)_2$ (**6**)	MeCN	−0.51 [a]	−0.96 [a]	−0.72	
$[Cu(NCMe)(L^2)](BF_4)_2$ (**7**)	MeCN	−0.17	−0.94 [a]	−0.68	
$[Cu(NCMe)(L^3)](BF_4)_2$ (**8**)	MeCN	−0.18	−0.91 [a]	−0.69	

Data were obtained in CH_2Cl_2/0.5 M $N^nBu_4PF_6$, dmf/0.1 M $N^nBu_4PF_6$ or MeCN/0.1 M $N^nBu_4PF_6$ at 298 K. Potentials are quoted vs. an internal ferrocene/ferrocenium standard, at scan rate 100 mV s^{-1}.

[a] Irreversible process, E_{pc} value quoted.

[b] Additional Pd-based reductions are also observed, at $E_{pc} = -1.6$, -2.0, -2.4 and -2.5 V.

propose dimeric $[\{Cu(\mu\text{-}Cl)L\}_2](BF_4)_2$ ($L = L^2$, L^3) structures in the solid state and in solution. Consistent with this, the EPR spectra of **5** and **6** closely parallel to those reported for salts of $[\{Cu(\mu\text{-}Cl)(terpy)\}_2]^{2+}$ have been previously reported [25]. In addition, the proposal of mononuclear structures for **7**–**9**, and dimeric structures for **5** and **6**, reconciles the anomalous relative d–d absorption energies of these two series of compounds (see above).

Voltammetric experiments were run in CH_2Cl_2/0.5 M $N^nBu_4BF_4$, MeCN/0.1 M $N^nBu_4BF_4$ or dmf/0.1 M $N^nBu_4BF_4$ at 298 K (Table 7). All potentials in the following discussion are quoted against an internal ferrocene/ferrocenium standard, and were measured at a scan rate of 100 mV s^{-1}. Both L^2 and L^3 are electrochemically inert in CH_2Cl_2 and MeCN within the available window for these solvents. In order to more accurately quantify the electrochemical behaviour that might be expected upon coordination of these ligands, the doubly protonated ligand $[H_2L^2](BF_4)_2$ was prepared by treatment of L^2 with three molar equivalents of HBF_4 in MeOH, and its electrochemical behaviour examined. This ligand salt exhibited a quasi-reversible reduction at $E_{1/2} = -0.92$ V in CH_2Cl_2. Hence, both metal- and ligand-based reactivity was anticipated in the voltammograms of **1**–**8**.

For solubility reasons, cyclic voltammograms (CVs) of **1**–**4** were run in dmf. The Pd(II) complexes **1** and **2** exhibit complex CVs, containing two principle processes: an irreversible reduction at $E_{pc} = -1.20$ V; and a more intense irreversible reduction at $E_{pc} = -2.5$ V, whose peak current is approximately twice that of the first reduction. Several other weak irreversible reductive waves also appear between these two values. We tentatively assign the first reduction to a L/L$^-$ ($L = L^2$, L^3) couple, owing to its proximity to the analogous reduction shown by **3** and **4** (see below), and the other reductions to Pd-based processes arising from decomposition products formed following this ligand reduction.

The CVs of **3** and **4** exhibit three *quasi*-reversible reductions (Fig. 4(a)). By analogy with the cyclic voltammogram of $[PtCl(terpy)]^+$, which contains three processes at similar potentials to those here [8], we assign the first reduction to a L/L$^-$ ($L = L^2$, L^3) couple. The second reduction may be a Pt(II/I) wave, although this was not definitively proven [8], while no assignment of the third reduction of $[PtCl(terpy)]^+$ has been made. Differential pulse voltammetry showed that the first

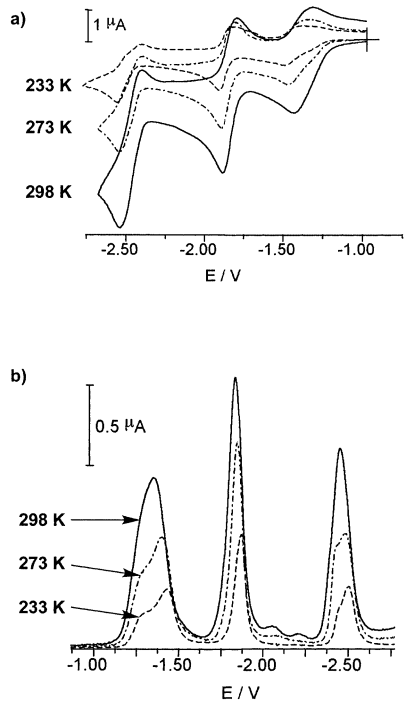

Fig. 4. (a) Cyclic voltammograms and (b) differential pulse voltammograms of $[PtCl(L^2)]BF_4$ (**3**) in dmf/0.1 M $N^nBu_4BF_4$ at 298, 273 and 223 K. The potential scale is referenced to the internal ferrocene/ferrocenium standard.

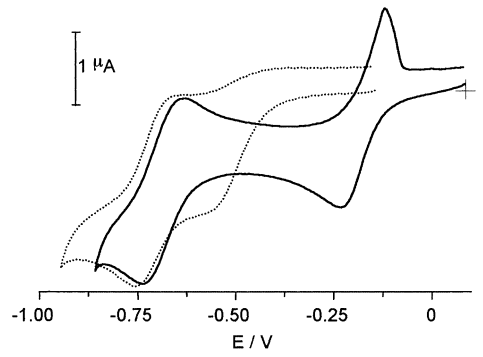

Fig. 5. Cyclic voltammograms of $[\{Cu(\mu\text{-}Cl)(L^2)\}_2](BF_4)_2$ (**5**, dashed line) and $[Cu(NCMe)(L^2)](BF_4)_2$ (**7**, solid line) in MeCN/0.1 M $N^nBu_4BF_4$ at 298 K. The potential scale is referenced to the internal ferrocene/ferrocenium standard. The irreversible third reduction exhibited by these compounds (Table 7) is not shown.

and third reduction waves actually contain two closely overlapping processes; this splitting becomes more pronounced at lower temperatures (Fig. 4(b)). Although such splitting was not detected in the CV of [PtCl(terpy)]$^+$ [8], it is known that [PtCl(terpy)]$^+$ and [PtCl(terpy)] both undergo monomer/dimer equilibria in solution with $K \approx 10\ M^{-1}$ [8]. Hence, we suggest that the overlapping reduction peaks for **3** and **4** correspond to reduction of monomeric and dimeric species at a given oxidation level.

We can make the following additional observations about the CVs of **3** and **4**. First, the assignment of the second reduction as a Pt-based process is supported by the lack of splitting on this peak. A Pt(II/I) reduction will involve insertion of an electron into a $d_{x^2-y^2}$ orbital, which lies perpendicular to the intradimer Pt···Pt vector and so will have essentially identical energies in the monomeric and dimeric species. Second, the observation of overlapping peaks on the third reduction wave of **3** and **4** both suggests its assignment as a ligand-based process, and implies that $[PtClL]^-$ (L = L^2, L^3) also exists as a mixture of monomers and dimers, with a similar equilibrium constant to those for the less reduced species.

Complexes **5**–**8** each exhibit three electrochemical reduction processes in MeCN (Table 7, Fig. 5). It is only the first of these that varies significantly between the compounds. For **5** and **6** this is an irreversible reduction, occurring near $E_{pc} = -0.55$ V; while for **7** and **8** a *quasi*-reversible wave is observed at $E_{1/2} = -0.18$ V. The latter process exhibits an abnormal lineshape, however, with an unusually sharp return wave that may be indicative of partial adsorption of the reduced species onto the electrode. The second and third reductions for **5**–**8** are essentially identical for all four compounds, occurring as a *quasi*-reversible wave at $E_{1/2} = -0.70 \pm 0.02$ V; and an irreversible peak in the range $E_{pc} = -0.95 \pm 0.04$ V. The most negative reduction exhibits a daughter desorption spike characteristic of the adsorption of Cu metal at the electrode.

On the basis of these data, and by analogy to the voltammetric behaviour of other Cu/terpyridyl complexes [26], the first, second and third reduction waves were, respectively, assigned to Cu(II/I), L/L^- (L = L^2, L^3) and Cu(I/0) reductions (Table 5). That the L/L^- and Cu(I/0) processes occur at essentially identical potentials for **5**–**8** suggests that initial reduction of **5** and **6** might lead to rapid dissociation of Cl^- from the Cu ions; this would also account for the irreversibility of this reduction for **5** and **6**. However, this hypothesis cannot account for the different Cu(I/II) reoxidation behaviour exhibited by the two sets of compounds. Hence, further experiments are required to quantify the structures of the reduction products of **5**–**8**, which might be monomeric or dimeric in nature [26,27].

Given that the CVs of **3** and **4** match that of [PtCl(terpy)]$^+$ very closely, it is interesting that **5**–**8** show an apparently ligand-based reduction at such a positive potential as -0.7 V, when other Cu/terpyridyl complexes exhibit irreversible terpy-based reduction reactions at $E_{pc} < -1.8$ V [26,28]. We note that, in all these literature cases, the ligand-based reduction potential is substantially anodic of the Cu(I/0) couple, and lies close to the reduction potential of the relevant non-coordinated terpyridine derivative. Hence, it appears that the unusually positive and reversible L/L^- (L = L^2, L^3) reductions shown by **5**–**8** reflect the fact that the ligand 'L' is still coordinated to Cu(I) ions when this reduction takes place. In the literature compounds, the more negative ligand-based reduction is of free terpyridine, decoordinated following reduction of the complex to metallic copper.

4. Concluding remarks

We have prepared a terpyridine derivative L^2, bearing a flexible 3-phenylpropoxy side chain that, in principle, could readily form an intramolecular π–π interaction with the terpyridine moiety that introduces little or no conformational strain onto the propoxy linker. Unfortunately, however, there is no evidence that such a π–π interaction is formed by L^2, or any of its complexes we have examined, in the solid state or in solution. Evidently the π–π interaction on its own, which is likely to have an enthalpy of no more than 20 kJ mol^{-1} [29], is insufficient to overcome other weak intermolecular interactions involving the terpyridine and/or phenyl groups that prevent it from forming. Hence, in order to accomplish our aim of preparing an intramolecularly π–π-stacked polypyridine, we must use a more rigid linker group that forces the polypyridine and aryl units to adopt a face-to-face geometry. We are actively pursuing this challenge.

5. Supplementary material

Crystallographic data for the structural analysis have been deposited with the Cambridge Crystallographic Data Centre, CCDC Nos. 164048 and 164049 for $1.2CH_3NO_2$ and **9**, respectively. Copies of this information may be obtained free of charge from The Director, CCDC, 12 Union Road, Cambridge, CB2 1EZ, UK (fax: +44-1223-336033; e-mail: deposit@ccdc.cam.ac.uk or www: http://www.ccdc.cam.ac.uk).

Acknowledgements

The authors gratefully acknowledge funding by The Royal Society (M.A.H.), the EPSRC (X.L.) and the University of Leeds.

References

[1] M.A. Halcrow, E.J.L. McInnes, F.E. Mabbs, I.J. Scowen, M. McPartlin, H.R. Powell, J.E. Davies, J. Chem. Soc., Dalton Trans. (1997) 4025.
[2] X. Liu, L.M.L. Chia, C.A. Kilner, L.J. Yellowlees, M. Thornton-Pett, S. Trofimenko, M.A. Halcrow, Chem. Commun. (2000) 1947.
[3] M. Matsumoto, Y. Inokuchi, K. Ohashi, N. Nishi, J. Phys. Chem. A 101 (1997) 4574.
[4] K. Ohashi, Y. Nakane, Y. Inokuchi, Y. Nakai, N. Nishi, Chem. Phys. 239 (1998) 429.
[5] (a) O. Yamauchi, A. Odani, J. Am. Chem. Soc. 107 (1985) 5938;
(b) O. Yamauchi, A. Odani, Inorg. Chim. Acta 100 (1985) 165;
(c) H. Masuda, T. Sugimori, A. Odani, O. Yamauchi, Inorg. Chim. Acta 180 (1991) 73;
(d) T. Sugimori, H. Masuda, N. Ohata, K. Koiwai, A. Odani, O. Yamauchi, Inorg. Chem. 36 (1997) 576;
(e) F. Zhang, T. Yajima, H. Masuda, A. Odani, O. Yamauchi, Inorg. Chem. 36 (1997) 5777;
(f) S. Ali, A. Sajadi, B. Song, H. Sigel, Inorg. Chim. Acta 283 (1999) 193;
(g) M. Mizutani, I. Kubo, K. Jitsukawa, H. Masuda, H. Einaga, Inorg. Chem. 38 (1999) 420.
[6] A. Odani, S. Deguchi, O. Yamauchi, Inorg. Chem. 25 (1986) 62.
[7] (a) K.W. Jennete, J.T. Gill, J.A Sadownick, S.J. Lippard, J. Am. Chem. Soc. 98 (1976) 6159;
(b) J.A. Bailey, M.G. Hill, R.E. Marsh, V.M. Miskowski, W.P. Schaefer, H.B. Gray, Inorg. Chem. 34 (1995) 4591.
[8] M.G. Hill, J.A. Bailey, V.M. Miskowski, H.B. Gray, Inorg. Chem. 35 (1996) 4585.
[9] M.D. Ward, E.C. Constable, J. Chem. Soc., Dalton Trans. (1990) 1405.
[10] G.M. Sheldrick, Acta Crystallogr., Sect. A 46 (1990) 467.
[11] G.M. Sheldrick, SHELXL-97, Program for the refinement of crystal structures, University of Göttingen, Göttingen, Germany, 1997.
[12] C.A. Hunter, J.K.M. Sanders, J. Am. Chem. Soc. 112 (1990) 5525.
[13] (a) G.R. Newkome, F. Cardullo, E.C. Constable, C.N. Moorefield, A.M.W. Cargill Thompson, J. Chem. Soc., Chem. Commun. (1993) 925;
(b) E.C. Constable, A.M.W. Cargill Thompson, P. Harveson, L. Macko, M. Zehnder, Chem. Eur. J. 1 (1995) 360;
(c) D. Armspach, M. Cattalini, E.C. Constable, C.E. Housecroft, D. Phillips, Chem. Commun. (1996) 1823;
(d) G.R. Newkome, E. He, J. Mater. Chem. 7 (1997) 1237;
(e) E.C. Constable, C.E. Housecroft, L.A. Johnston, D. Armspach, M. Neuburger, M. Zehnder, Polyhedron 20 (2001) 483.
[14] M.A. Halcrow, E.K. Brechin, E.J.L. McInnes, F.E. Mabbs, J.E. Davies, J. Chem. Soc., Dalton Trans. (1998) 2477.
[15] (a) T. Rojo, J. Darriet, J.M. Dance, D. Beltran-Porter, Inorg. Chim. Acta 64 (1982) L105;
(b) T. Rojo, M.I. Arriotua, J. Ruiz, J. Darriet, G. Villeneuve, D. Beltran-Porter, J. Chem. Soc., Dalton Trans. (1987) 285.
[16] (a) P. Castan, F. Dahan, S. Wimmer, F Wimmer, J. Chem. Soc., Dalton Trans. (1990) 2679;
(b) W. Zhang, C. Bensimon, R.J. Crutchley, Inorg. Chem. 32 (1993) 5808.
[17] M. Howe-Grant, S.J. Lippard, Inorg. Synth. 20 (1980) 101.
[18] K. Nakamoto, Infrared and Raman Spectra of Inorganic and Coordination Compounds, Part B, 5th ed., Chichester, Wiley, 1997, pp. 113–115.
[19] (a) G.M. Intille, C.E. Pfluger, W.A. Baker Jr., J. Cryst. Mol. Struct. 3 (1973) 47;
(b) P. Castan, F. Dahan, S. Wimmer, F.L. Wimmer, J. Chem. Soc., Dalton Trans. (1990) 2679;
(c) R.E. Rülke, I.M. Han, C.J. Elsevier, K. Vrieze, P.W.N.M. van Leeuwen, C.F. Roobeek, M.C. Zoutberg, Y.F. Wang, C.H. Stam, Inorg. Chim. Acta 169 (1990) 5;
(d) W.G. Zhang, C. Bensimon, R.J. Crutchley, Inorg. Chem. 32 (1993) 5808;
(e) S. Ramdeehul, L. Barloy, J.A. Osbourn, A. De Cian, J. Fischer, Organometallics 15 (1996) 5442.
[20] (a) O.P. Anderson, A.B. Packard, M. Wicholas, Inorg. Chem. 15 (1976) 1613;
(b) I. Castro, J. Faus, M. Julve, M. Philochelevisalles, Transition Met. Chem. 17 (1992) 263;
(c) C-C. Su, C-B. Li, Polyhedron 13 (1994) 825;
(d) V. Bulach, H. Duval, J. Fischer, R. Weiss, Acta Crystallogr., Sect. C 53 (1997) 543;
(e) J. Pickardt, B. Staub, K.O. Schafer, Z. Anorg. Allg. Chem. 625 (1999) 1217;
(f) G. Francese, H.W. Schmalle, S. Decurtins, Acta Crystallogr., Sect. C 55 (1999) 730.
[21] L. Pauling, The Nature of the Chemical Bond, 3rd ed., Cornell University Press, Ithaca, NY, 1960, pp. 257–264.
[22] W.J. Geary, Coord. Chem. Rev. 7 (1971) 81.
[23] D.W. Shriver, P.W. Atkins, Inorganic Chemistry, 3rd ed., Oxford University Press, Oxford, UK, 1999, p. 228.
[24] B.A. Goodman, J.B. Raynor, Adv. Inorg. Chem. 13 (1970) 135.
[25] J.V. Folgado, E. Coronado, D. Beltrán, J. Chem. Soc., Dalton Trans. (1986) 1061.
[26] (a) A.L. Crumbliss, A.T. Poulos, Inorg. Chem. 14 (1975) 1529;
(b) K.T. Potts, M. Kesharvaz-K, F.S. Tham, H.D. Abruña, C. Arana, Inorg. Chem. 32 (1993) 4450;
(c) G.D. Storrier, S.B. Colbran, D.C. Craig, J. Chem. Soc., Dalton Trans. (1998) 1351;
(d) M.A. Halcrow, E.K. Brechin, E.J.L. McInnes, F.E. Mabbs, J.E. Davies, J. Chem. Soc., Dalton Trans. (1998) 2477.
[27] (a) E.C. Constable, A.J. Edwards, M.J. Hannon, P.R. Raithby, J. Chem. Soc., Chem. Commun. (1994) 1991;
(b) E.C. Constable, T. Kulke, M. Neuburger, M. Zehnder, Chem. Commun. (1997) 489.

[28] N.W. Alcock, P.R. Barker, J.M. Haider, M.J. Hannon, C.L. Painting, Z. Pikramenou, E.A. Plummer, K. Rissanen, P. Saarenketo, J. Chem. Soc., Dalton Trans. (2000) 1447.
[29] (a) S.K. Burley, G.A. Petsko, Science 229 (1985) 23;
(b) S.B. Ferguson, E.M. Seward, F. Diederich, E.M. Sanford, A. Chou, P. Inocencio-Szweda, C.B. Knobler, J. Org. Chem. 53 (1988) 5593;
(c) W.L. Jorgensen, D.L. Severance, J. Am. Chem. Soc. 112 (1990) 4768;
(d) J. Zhang, J.S. Moore, J. Am. Chem. Soc. 114 (1992) 9701.